

# Contact Distance Estimation by a Soft Active Whisker Sensor Based on Morphological Computation

Nhan Huu Nguyen<sup>1</sup>, Trung Dung Ngo<sup>2</sup>, Dinh Quang Nguyen<sup>1</sup>, and Van Anh Ho<sup>1</sup>

**Abstract**—Mammals use whiskers to sense their surrounding environments. By whisking over an object to transduce tactile signals (forces or moments) to mechanoreceptors at the snout, then transmitting this data to the somatosensory cortex in the brain, they can extract features such as contact distance, texture and shape of the object. In this study, we propose a morphological computation method to localize the contact position/locate the contacted object by investigating the induced strain, measured by a strain gauge representing sensory nerves, along the length of a whisker. To accomplish this task, an artificial tapered whisker sensor was made from a soft material (silicon rubber) to provide flexibility, sensitivity and more importantly adaptability. The first part of this paper introduces an analytical model of the proposed whisker based on elastic linear beam theory, and describes the unique correlations among the strain, contact distance, and whisker movements. The second part of this paper analyzes differences between the analytical model and a practical model to ascertain the optimum sensing conditions and any similarities in tactile behavior among the proposed whisker and a biological one. Our final goal is to give an idea of simple soft whisker-like sensory system which can be integrated in an autonomous robot.

## I. INTRODUCTION

Rodents burrow and inhabit dark narrow constrained spaces. The mystacial vibrissae (whisker) sensory system is a vital organ that helps such animals perform activities precisely. Many studies have investigated the working principle of mammal whiskers collecting tactile information. For instance, rats move their whiskers back and forth through the space surrounding the head to localize and "feel" features of objects [1]-[4]. In attempt to mimic this ability, there has been increasing interest in constructing a whisker system, especially for mobile robots [5][6]. A soft artificial whisker is promising to provide mobile robots flexible tactile capacity for a mobile robots to avoid obstacles in environmental surrounding and identify its fellow in the swarm as shown in figure 1. In order to accomplish this task, detecting contact distance, which indicates the distance from the contact point to the rotational axis in a reference coordinate system represented by the term  $a$  in Fig. 1, is the most fundamental application of an artificial whisker. By collecting a set of contact points over a whisking period, information regarding the texture and shape of the object can be constructed.

Biological and behavioral experiments have demonstrated that rats explore objects with tactile signals directly trans-

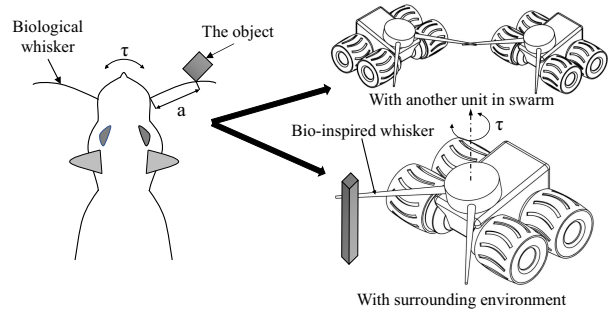


Fig. 1. Artificial whisker sensor system mimicking the tactile perception behaviors of the biological whisker from rodents such as rats.

duced to a follicle-sinus complex (beneath the skin) which contains hundreds of mechanoreceptors. Until now, studies on utilization of morphological change of the whisker at different stages of the sensing process are lacking. In this study, we investigated the mechanical variable called strain indicating change in perpendicular length of a whisker after making contact (Fig. 2(b)). Furthermore, evidence that sensing elements of an insect antenna are located along its length, has been established [7].

Here, we propose an effective design for a soft artificial whisker with ability to sense contact information from a sensing element (strain gauge) located along the whisker length. This approach is especially appropriate for analyzing the morphology of the whisker during active whisking to determine the location of the contact point. Our results demonstrate the significant role of whisker morphology in object localization and more importantly in selecting the most appropriate sensing strategy for a specific task. The main outcomes can be summarized as follows:

- 1) We proposed an idea and constructed a prototype model silicon-rubber whisker sensing system with a strain gauge which assesses the morphology of the whisker.
- 2) We used a linear beam theory to analyze responses of the sensing system model associated with morphological change during active sensing.

## II. BACKGROUND

### A. Artificial whisker inspiring from biological creatures

Emmett *et al.* in [8] conducted a preliminary analysis of a whisker as a cantilever beam and suggested that an information set comprising three components of force/moment is sufficient to estimate contact point location in 3D space. An

<sup>1</sup>Authors are with the School of Material Science, Japan Advanced Institute of Science and Technology (JAIST), 1-1 Asahidai, Nomi, Ishikawa, 923-1292 Japan. s1920009@jaist.ac.jp

<sup>2</sup>Trung Dung Ngo is with the Faculty of Sustainable Design Engineering, University of Prince Edward Island, 550 University Ave, Charlottetown Prince Edward Island, Canada

artificial whisker-follicle complex was developed to draw a spatial map of all force/moment components generated by contact force in different terrains. Though, this idea was actually proposed by Kaneko *et al.* [9] who had the idea of correlating the curvature of the whisker and the mechanical torque at the base by introducing the term *Rotational compliance* which denotes resistance of the whisker against protraction movement. Mat Evans *et al.* [10], Kim and Moller [11] proposed similar designs to each other for a robot whisker using a magnetic sensor (Hall effect sensor) located near its base. During interaction, a whisker may be considered a mechanical oscillator wherein amplitude and velocity of whisker vibration brings tactile information to the follicle [1][12]. Recently, there have been many studies mimicking whisker ability of not only determining contact but predicting it from pre-contact air or water pressure similar to the ability of seals [13]. This might enable an aquatic or flying robot to analyze ocean currents or air streams.

However, a comprehensive sensing system embedded at the whisker base would occupy much space in a robot, especially if there were an array of whiskers. One might overcome this limitation by removing redundancy to use artificial follicles for specific purposes. Another limitation may be a threshold limit of artificial mechanoreceptors when interaction is near the receptors or the whisker bending angle is small [14]. Our method of using a strain gauge to observe morphological change has overcome these limitations. Another aspect to be considered is the fabrication material. Most existing designs tend to fabricate whiskers from steel or aluminum wire. soft material (silicon-rubber) will bring flexibility of movement and more importantly adaptability which is crucial for autonomous robots.

### B. Sensing strategy

Many neurophysiological and behavioral studies have shown that rodents apply two different sensing strategies: active sensing and passive sensing [15][16]. Passive sensing is when a whisker moves linearly forward to an object instead of sweeping over it. Williams *et al.* [14] suggested such passive stimulation is to prevent an accidental collision or assault from the surrounding environment. An experimental simulation [15] indicated that rodents cannot detect angular displacement which is crucial to measure any kind of mechanical variable.

Active sensing overcomes most disadvantages of passive sensing and seems more appropriate for object feature extraction. Furthermore, the active sensing strategy increases spatial acuity of the whisker with a wider range of whisking angle. Thus, in this paper, we only focus on active sensing. Nevertheless, it is worth noting that our method may be also applied for passive sensing strategy. Regarding active sensing, behavioral data recently suggested that rats tend to tap their whiskers against rather than sweep them over an object to detect the contact location [15][16]. That means the most accurate distance extraction can be gained in the very early stage after making contact. The term

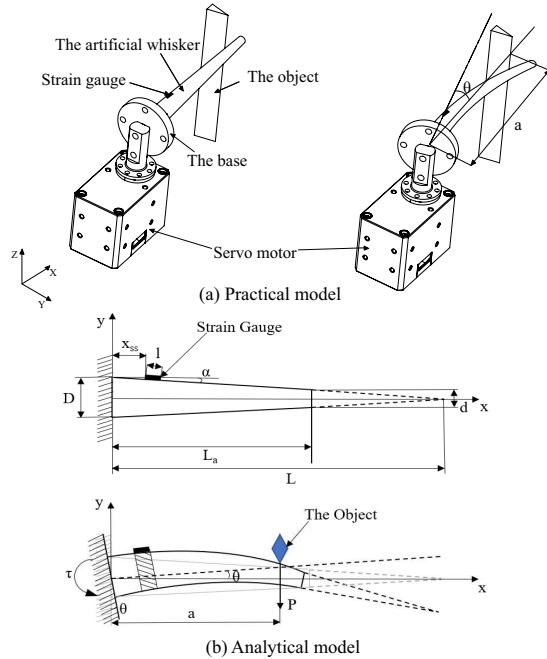


Fig. 2. (a) The schematic drawings of the active whisker sensor system, (b) Morphology analysis of the whisker during interaction

called *Minimum impingement strategy* [17] is used to indicate this particular feature. In general, we can distinguish these sensing abilities based on angular displacement of the whisker. Sweeping motion is perceived as more suitable for texture and shape of an object due to a larger range of angular displacement. In the next sections, we introduce an investigation of morphological change in selecting sensing ability.

## III. MATERIALS AND METHODS

### A. Design of the Whisker Prototype

The most common and simplest design for an artificial whisker is a solid cantilever beam. Consider a straight, homogeneous, flexible and linearly tapered whisker as a truncated cone with one end fixed at the base and other free as shown in Fig. 2(b). An artificial whisker of length \$L\_a\$ rotates through angle \$\theta\$ against the surface of an object at distance \$a\$. In which, \$L\$, \$D\$ and \$d\$ are original length, diameter of the base and diameter of the tip of the whisker, respectively. To sense the strain at a certain position \$x\_{ss}\$ distance from the base, a strain gauge, with grid length (strain sensing part) \$l\$, is bonded in the direction that principal strain is measured from the sensing plane (the plane of rotation).

### B. Deflection of the whisker during whisking

Figure 2(b) shows a model mimicking rat behavior of continuously whisking back and forth until a whisker contacts with an object. The whisker base is actuated in a single axis by a servo motor with constant velocity resulting in bending angle \$\theta\$, which is taken equivalently as the term *angular displacement*. We developed an accurate but simple analytical whisker model using classical elasticity beam theory

Euler-Bernoulli [17] to obtain a unique correlation between contact distance and moment at a certain position from the base as:

$$\kappa(x) = \frac{d^2y}{dx^2} = \frac{M(x)}{EI(x)}, \quad (1)$$

where

$$M(x) = P \times (a - x),$$

$$I(x) = \frac{\pi d^4(x)}{64} = \frac{\pi D^4(L - x)^4}{64L^4}. \quad (2)$$

In equation (1),  $d^2y/dx^2$  is the second derivative of the deflection of the whisker with respect to arbitrary position  $x$  along the whisker.  $M(x)$ ,  $I(x)$  and  $d(x)$  are the internal moment, the second moment and varied diameter of section area, respectively,  $E$  is Young's modulus and varied dependently on the contact force which is proportional to angular displacement. The term  $EI(x)$  is also called flexural rigidity since it is a measure of the resistance of the beam to deflection. Before further discussing the model analysis, an essential list of assumptions needs to be made as follows:

- a. The target object is rigid and stationary during active sensing.
- b. The whisker model is considered initially straight, homogeneous and its deflection is only through small angles  $\theta$  ( $\sim 10^\circ$ ) to ensure linear approximation equation (1) is applicable.
- c. Lateral slip is assumed absent during active sensing.
- d. The curvature of the surface is within the sensing plane.
- e. The whisker is assumed to make contact with a single point or an edged environment.

Substituting the expansion form of  $M(x)$  and  $I(x)$  in equation (1) and taking integration twice to obtain the deflection at the contact point  $a$  gives:

$$y(x) = \frac{32PLx^2}{3\pi ED^4} \left[ \frac{3La - Lx - 2ax}{(L - x)^2} \right]. \quad (3)$$

Replacing  $x = a$  and  $y(x) = a \tan \theta \approx a\theta$ , due to the assumption b, into equation (3):

$$\theta = \frac{64PL}{3\pi ED^4} \frac{a^2}{L - a} \quad (4)$$

In short, in an active whisker sensor system, if terms  $P$  and  $\theta$  are given, contact distance  $a$  can be directly determined by solving Eq. (3). However, it essentially requires a sensing device to detect the torque/moment at the base, which makes the model more sophisticated and accounts for noise among the tactile information. In the next section, by introducing an algorithm to calculate the strain, which is also dependent on material characteristics, Young's modulus is expected to be canceled out.

### C. Strain analysis

Strain  $\varepsilon$  (a dimensionless quantity) is defined as the ratio of deformation in length to the original (i.e.  $\varepsilon = \frac{\Delta L}{L}$ ) caused by elongation or compression force. Let us assume that Hooke's Law is applicable to our model. Thus, the

relationship between stress  $\sigma$  and strain  $\varepsilon$  based on Hooke's Law can be expressed as follows:

$$\varepsilon = \frac{\sigma}{E}. \quad (5)$$

According to Fig. 2(b),  $\varepsilon$  is the total strain measured from the area beneath the strain gauge, and  $\sigma$  is the sum of stress generated by bending force. Equation (5) can be rewritten as follows:

$$\varepsilon = \frac{\sigma}{E} = \frac{y \sum M(x)}{E \sum I(x)}, \quad (6)$$

where  $y$  is the distance from the neutral axis to the extreme fiber where the strain was measured ( $y = \frac{d(x)}{2}$ ). By substituting  $M(x)$  and  $I(x)$  from Eq. (2) into (6), the final form of Eq. (6) is given as:

$$\varepsilon = \frac{32PL^3}{E\pi D^3} \int_{x_{ss}}^{x_{ss} + l \cos \alpha} \frac{a - x}{(L - x)^3} dx, \quad (7)$$

where  $x_{ss}$ ,  $l$  are distances from the base to the sensing part of the strain gauge and grid length, respectively. The term  $\alpha$  is the geometrical feature of the model described in Fig. 2(b). Combining equation (4) and (7) gives:

$$\varepsilon = \frac{3DL^2}{2} \frac{\int_{x_{ss}}^{x_{ss} + l \cos \alpha} \frac{a - x}{(L - x)^3} dx}{\left[ \frac{a^2}{L - a} \right]} = f(a). \quad (8)$$

Equation (8) implies that: 1) Contact distance  $a$  is linearly proportional to the ratio of amplitude of strain gauge  $\varepsilon$  and angular displacement  $\theta$ . 2) As expected, the expression of Eq. (8) has already canceled out Young's modulus  $E$  and contact force  $P$  which is one of the critical advantages of this study. In other words, from now on, the morphology of the whisker is described by the term *Strain* including variation of material property. As mentioned in [15], it seems likely that animals can feel only *feel* rate of change of tactile information rather than determine its absolute value.

### D. Soft material characterization

The variation of material properties must be taken into account of morphological computation along with the change in geometry. To clarify this issue, we consider the basic curve of stress (directly related to the contact force or moment) compared to the strain for silicon-rubber during elongation. Generally, the stress-strain curve of silicon rubber has an unusual shape. The curve may comprise two regions I and II as illustrated in Fig. 3. When the whisker starts making contact with the object, the ratio of stress from the strain is a constant corresponding to the region I. Thus, Hooke's law is valid within this proportionally limit, in the other words, the strain conversion factor will remain relatively unchanged (Young's modulus remains constant) as long as the applied force/moment is small. In contrast, its linearity ceases along the increase of strain, large strain is observed with small increases in stress and the gradient of the graph decreases ( $E$  decreases) in region II. Consequently, the change of  $E$

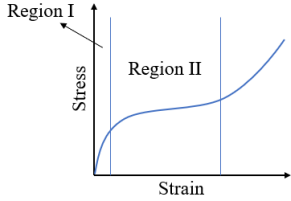


Fig. 3. The fundamental strain-stress curve of silicon-rubber for elongated stage only

will be identified as the term  $K$  based on Hook's law as follow:

$$\frac{\varepsilon_m \times K}{\theta} = f(a) \Rightarrow K = \frac{\theta}{\varepsilon_m} \times f(a) \quad (9)$$

Once  $K$  factor is identified, the contact distance can be directly calculated through the equation (8).

#### IV. EXPERIMENTS AND DISCUSSIONS

To assess the reliability of the method and whisker design proposed in this paper, we made and tested three prototypes. The models had the base diameter ( $D = 10$  mm), sensor position ( $x_{ss} = 5$  mm), and whisker length ( $L_a = 50$  mm) but different diameter tips ( $d_1 = 4$  mm,  $d_2 = 7$  mm,  $d_3 = 10$  mm). By analyzing strain gauge amplitude for each model, we expect not only to understand more about how rodents actively choose sensing ability based on morphology, but suggest the optimum measuring conditions and whisker design to sense tactile information with the highest precision. A DC servo motor (DYNAMIXEL XH430-W350-R) was used to rotate the whisker. The measured database obtained by a measuring instrument (EDX-15A) connected with a bridge box (UI-54A-120) was sent to a computer and analyzed by data acquisition system DCS-100A (Kyowa Electronic Instrument Co.) and MATLAB R2019a.

##### A. Process for fabrication of experimental whiskers

The whisker models were fabricated by a casting process using rubber (Smooth-sil 960, Smooth-on Inc., PA, USA.). The casting molds were designed by CAD software Solidworks and printed using a 3D printer (Zortrax M200, Zortrax, Olsztyn, Poland). The sensor system including the base and the whisker models after curing are shown in Fig. 4(a),(b). After fixing the whiskers to the bases, the sensor position  $x_{ss}$  was marked then the strain gauge attached by glue and covered by a thin layer of silicon glue. Equation (7) demonstrates that the strain gauge should be placed as close as possible to the base to amplify the signal. The strain gauge used in this paper was KFGS-2-120-C1-11 L1M2R from Kyowa Electronic Instrument Co., with gage factor  $G = 2.21$ , grid length  $l = 2$  mm and was bonded by adhesive glue CC-33A.

##### B. Validation for analytical model

We conducted a experimental test to observe the tactile signal of the strain gauge  $\varepsilon_m$  under different measuring conditions (i.e. varied contact distance  $a_i$  along the whisker

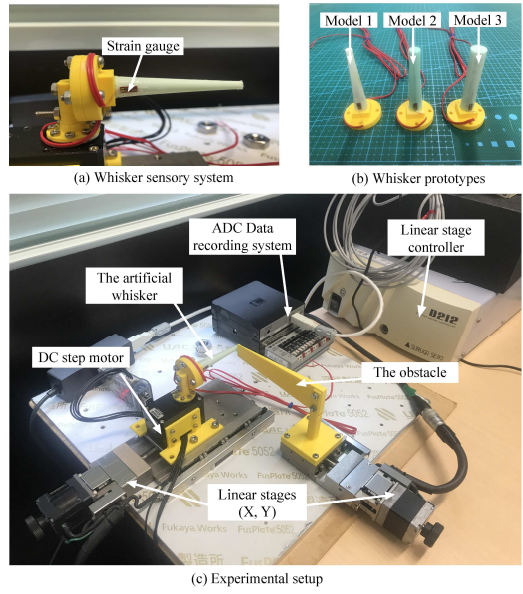


Fig. 4. (a) The design and printed mold for the whisker, (b) The artificial whiskers (tip diameters are 4 mm, 7 mm and 10 mm, respectively from the left to right), and (c) Experimental setup include two linear stages in X, Y direction in which a stage carries DC servo motor with the artificial whisker attached on it, another one carries the obstacle. Those linear stages will be controlled by the controller.

length and different angular displacements  $\theta_i$ ) to compare with the analytical model through Eq. (8). Figure 5(a) shows strain-angular displacement curves for the analytical and practical models for a surface contact point at same distance  $a$ . Similarly, figure 5(b) describes strain-contact position curves for specific angle  $\theta$ . The feasibility of substituting the value of strain gauge  $\varepsilon_m$  into Eq. (8) to calculate the contact distance can be justified. Moreover, the significant influence of the factor  $K$  have been shown clearly. In which,  $K_i$  and  $K_j$  represent the calibration factor with respect to varied contact distance and angular displacement as illustrated in Fig. 5. Whereas,  $K_j$  showed only a slight difference between two models when angle  $\theta$  was small, suggesting the proposed whisker is effective. In this study, we assume that the other reasons contributing in factor  $K$ , misalignment effect caused by inadequacy in the bonding procedure are negligible.

The linear stages will bring the object into slight contact with the whisker at arbitrary positions along the length  $a_{i=1 \sim 10} = [21, 24, 27, 30, 33, 36, 39, 42, 45, 48]$  mm. The experiments did not involve the tip of the whisker to avoid slippage, and the tip has previously proven inappropriate for this task [8]. For each case of  $a_i$ , the motor actuated the whisker to tap successively at angle  $\theta_{j=1 \sim 11} = [0.5, 1, 2, 3, 4, 5, 6, 7, 8, 9, 10]$  deg. For each pair of  $(a_i, \theta_j)$ , the signal from the strain gauge was recorded for signal post-processing which is introduced in the next section.

##### C. Variation of strain conversion factor $K$

From the experiment data, we calculated the value of factor  $K_{ij}$  for each whisker according to contact distance  $a_i$  and angular displacement  $\theta_j$ . The results are plotted in Fig. 6. It can be seen that all graphs share a similar gradient wherein

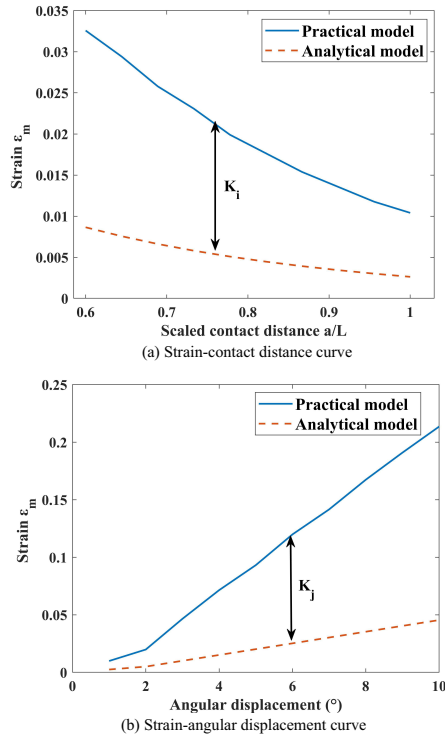


Fig. 5. Strain amplitude depending on, (a) distance and (b) angular displacement in the practical model compared to the analytical model (data for large protraction angles will be delegated for sweeping strategy)

the value of  $K$  shows a significant decrease when angular displacement  $\theta$  increases as well as when the stimulated location approaches the base. To determine the optimum tactile condition (among the surveyed values of  $\theta_j$ ) to detect the contact distance with the highest precision, we utilized the *Standard deviation – based algorithm* to assess how wide the value of  $K_j$  spread about the average. In other words, the larger the standard deviation (SD) the greater the error rate in tactile perception will be, for a specific angle of  $\theta_j$ .

Figure 7 plots variation of SD with angular displacement  $\theta_j$  in our whisker models. The figure trends are generally similar to each other. In general, the SD for whisker prototype 1 ( $d_1 = 4\text{ mm}$ ) is intuitively highest and seems to peak before the other two. This result is not surprising because the radius (and hence robustness against bending deformation) of model 1 at every point is smaller than that of other models. An similar conclusion may be reached upon comparing prototypes 2 ( $d_1 = 7\text{ mm}$ ) and 3 ( $d_1 = 10\text{ mm}$ ). Figure 7 implies that our model is can sense any contact distance along length  $L_a$  with the highest accuracy rate as long as it taps the object at a small angle.

#### D. Experiment procedure for contact localization using tapping strategy

To test this hypothesis, an experiment determining contact distance with varied angular displacement using tapping strategy was conducted. The results are summarized in Fig. 8. Contact distance was calculated by substituting the mean

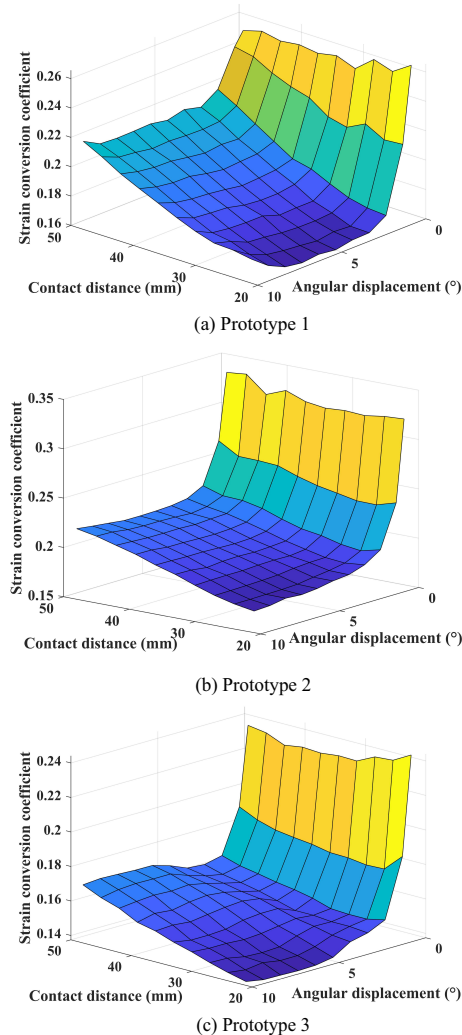


Fig. 6. The variation of the strain conversion factor  $K$  for (a) prototype 1, (b) prototype 2, (c) prototype 3. The presented figures show the same trend which gets smaller when the contact location is closer to the base, as well as the angular displacement is smaller. This non-linearity might affect to the tactile signal and the behaviors of theoretical or even natural whisker for a specific sensing capability.

value of  $K$  which is identified from results in section IV. C and the amplitude of strain gauge for each specific angle  $\theta_j$  into Eq. (9) then by making comparisons with the actual contact location. To start the test, the whisker makes slight contact with the object and continues rotating at the following angle of  $\theta_j$ . The contact distance is directly measured by substituting the mean value  $\bar{K}_j$  and strain amplitude corresponding to each case into Eq. (9). It is noticeable that the absolute value of the sensor should be equivalent when contact occurs at both sides of the whisker within the sensing plane.

Fig. 8 demonstrate the effectiveness of the whisker models using the tapping strategy in sensing distance information by inspecting the strain according to a specific angular displacement. As expected, error estimation in case of  $\theta_1 = 0.5\text{ deg}$  is the smallest, and gradually increases with  $\theta_1$ .

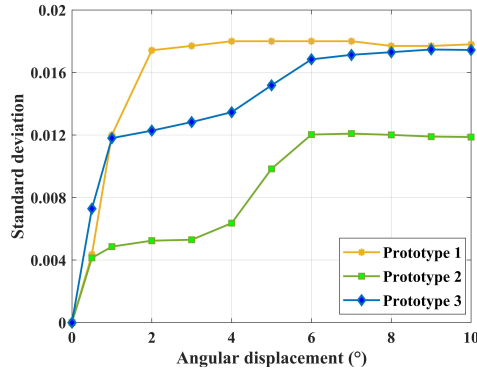


Fig. 7. The standard deviation of  $K$  for each whisker model (a) prototype 1, (b) prototype 2, (c) prototype 3. In the way stated from Fig. 4, if only the variation of  $K$  for each angle  $\theta_j$  is considered, it is clearly seen that small angle will provide the most *stable* tactile information (smallest standard deviation value) in order to detect contact point.

## V. CONCLUSION

This paper addressed the idea of a soft active whisker sensor able to localize the environment based on observation of morphological change in the whisker during interaction. From the discussion above, this is promising to develop an efficient solution to discriminate texture and shape in a 3D working space. It is expected to be improved by affixing another strain gauge perpendicular to the one in the present model. With the notion of using multiple strategies to sense different types of information, a practical experiment could be conducted to test how the artificial whisker adapt and adjust their behavior appropriately.

## REFERENCES

- [1] M. E. Diamond, M. V. Heimendahl, and E. Arabzadeh, "Whisker-mediated texture discrimination", *PLoS Biology*, Vol. 6, No. 8, pp. e220, 2008.
- [2] V. Hayward, "Is there a "plenoptic" function?", *Philos. Trans. R. Soc. B Biol. Sci.*, Vol. 366, No. 1581, pp. 3115–3122, 2011.
- [3] J. E. Bernth, V. A. Ho, and H. Liu, "Morphological computation in haptic sensation and interaction: from nature to robotics", *Adv. Robot.*, Vol. 32, No. 7, pp. 340–362, 2018.
- [4] B. Mitchinson, C. J. Martin, R. A. Grant, and T. J. Prescott, "Feedback control in active sensing: Rat exploratory whisking is modulated by environmental contact", *Proc. R. Soc. B Biol. Sci.*, Vol. 274, No. 1613, pp. 1035–1041, Apr. 2007.
- [5] A. Vaish, S. Y. Lee, and P. V. y. Alvarado, "Mechanical Fourier transform using an array of additively manufactured soft whisker-like sensors", in *2019 International Conference on Robotics and Automation (ICRA)*, 2019, pp. 9410–9415.
- [6] D. E. Kim and R. Möller, "Biomimetic whiskers for shape recognition", *Rob. Auton. Syst.*, Vol. 55, no. 3, pp. 229–243, 2007.
- [7] M. I. Zhukovskaya and A. D. Polyanovsky, "Biogenic amines in insect antennae", *Front. Syst. Neurosci.*, Vol. 11, p. 45, Jun. 2017.
- [8] H. Emmett, M. Graff, and M. Hartmann, "A novel whisker sensor used for 3D contact point determination and contour extraction," 2018.
- [9] M. Kaneko, N. Kanayama, and T. Tsuji, "Active antenna for contact sensing", *IEEE Trans. Robot. Autom.*, Vol. 14, No. 2, pp. 278–291, 1998.
- [10] M. H. Evans, C. W. Fox, N. F. Lepora, M. J. Pearson, J. C. Sullivan, and T. J. Prescott, "The effect of whisker movement on radial distance estimation: a case study in comparative robotics", *Front. Neurorobot.*, Vol. 6, No. January 2012, 2013.
- [11] D. E. Kim and R. Möller, "Biomimetic whisker experiments for tactile perception", *Proc. Int. Symp. Adapt. Motion*, pp. 1–7, 2005.

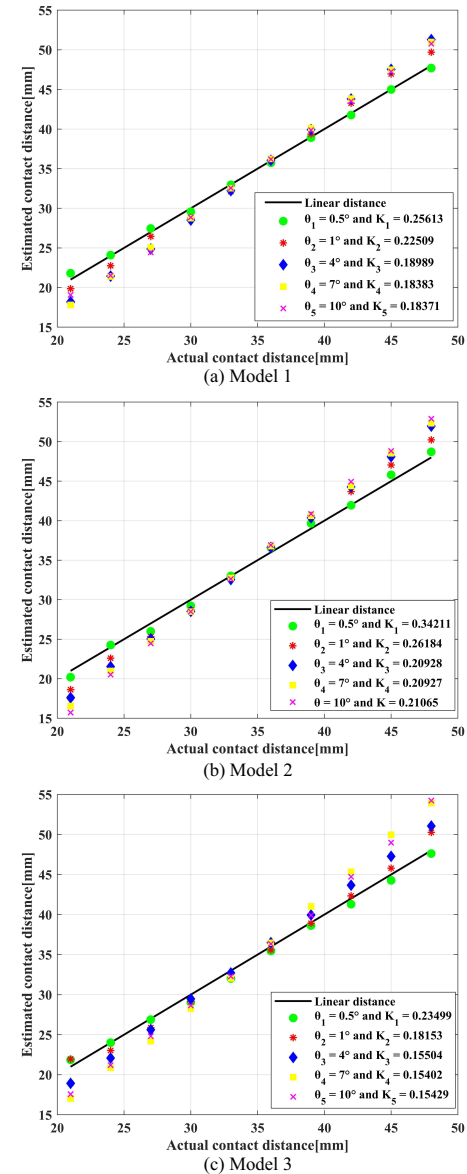


Fig. 8. Contact distance estimation based on the strain signal responding to five different angular displacements  $\theta$  ( $\theta_j=1\sim 5 = [0.5, 1, 4, 7, 10]$  deg) and the strain conversion factors  $K$ . (a) Tip diameter of  $d_1 = 4$  mm, (b)  $d_2 = 7$  mm and (c)  $d_3 = 10$  mm

- [12] E. Lottem and R. Azouz, "Mechanisms of tactile information transmission through whisker vibrations", *J. Neurosci.*, Vol. 29, No. 37, pp. 11686 LP – 11697, Sep. 2009.
- [13] W. Deer and P. E. I. Pounds, "Lightweight whiskers for Contact, pre-contact, and fluid velocity sensing", *IEEE Robot. Autom. Lett.*, Vol. 4, No. 2, pp. 1978–1984, 2019.
- [14] C. M. Williams and E. M. Kramer, "The advantages of a tapered whisker", *PLoS One*, vol. 5, no. 1, 2010.
- [15] J. A. Birdwell et al., "Biomechanical models for radial distance determination by the rat vibrissal system", *J. Neurophysiol.*, Vol. 98, No. 4, pp. 2439–2455, 2007.
- [16] J. H. Solomon and M. J. Z. Hartmann, "Radial distance determination in the rat vibrissal system and the effects of Weber's law", *Philos. Trans. R. Soc. B Biol. Sci.*, Vol. 366, No. 1581, pp. 3049–3057, 2011.
- [17] O. A. Bauchau and J. I. Craig, "Euler-Bernoulli beam theory BT - Structural Analysis", O. A. Bauchau and J. I. Craig, Eds. Dordrecht: Springer Netherlands, 2009, pp. 173–221.